

Research on tracking of maneuvering multi-target based on bionics forIRST system

Hui Chen · Chongzhao Han · Yuchun Zhang

Published online: 4 January 2011
© Springer Science+Business Media, LLC 2010

Abstract This paper mainly studies bearing-only target tracking based on bionics forIRST system. Some solutions for the key problem are presented in order to apply in an actual bearing-only engineering system. They include sensor technology, measurement pretreatment technology, association gate technology, data association technology, state filtering technology, etc. The premise of these new approaches is designing an effective sensor system which can reliably search and track targets in a large range. Then, it is important to improve the confirming efficiency of the real target and limit false track overextension with the dense clutter. Then, tracking processing needs a precise target initialization information and association information between the existing target and isolated measurement. At the same time, the threat level of the bearing-only target needs to be estimated based on limited bearing-only information. Finally, aiming at unrecognized model and complex maneuvering motion for bearing-only target in polar coordinates, an effective approach of state filtering algorithm with appropriate computation cost will be given. The application of the proposed approach in an actual engineering system proves its effectiveness and practicability.

H. Chen (✉) · C. Han
Institute of Integrated Automation, School of Electronic and Information Engineering, Xi'an Jiaotong University, Xi'an, China
e-mail: huich78@hotmail.com

C. Han
e-mail: czhan@mail.xjtu.edu.cn

H. Chen
Key Laboratory of Gansu Advanced Control for Industrial Processes, Lanzhou University of Technology, Lanzhou, China

Y. Zhang
School of International Economic and Management, Lanzhou University of Technology, Lanzhou, China
e-mail: nanhangzhyuch@163.com

Keywords Bionics · Target tracking · Bearing-only · Multi-model · Threat level

1 Introduction

Search and location by using bearing-only information with an IRST system increasingly becomes a major research domain [1–6] because it can be applied to any radiant source and it has no special requirement for the sensor system. IRST system tracks a target as a point, and its action distance is far enough. Different from other passive detection equipment, its angular resolution is much higher. It has a capacity of multi-target searching and tracking and has a significant advantage when dealing with much more intensive formation of a target. Therefore, it is widely used in ship-borne and airborne warning systems. By processing the angle measurement received by the IRST system, more accurate orientation information of radiation source is available, which is provided to the information center where the analysis of target threat level and attribute is finally completed. It is worth mentioning that a driving location device to obtain distance information with the help of this bearing-only filtered information would help to improve the overall performance of a target tracking system. On the other hand, with less available information of bearing-only tracking, modeling is difficult, highly nonlinear, and it is difficult to meet the precision of the filtering, and so on; this issue is extremely challenging around the world. This paper presents some solutions for bearing-only tracking of maneuvering multi-target based on bionics with IRST system. It includes sensor technology, measurement pretreatment technology, association gate technology, data association technology, state filtering technology, etc. Data association was already mentioned in detail in [6], and so we do not mention it in this paper.

2 Sensor system based on bionics

2.1 Design of sensor system

For a single passive sensor system, an IRST system realizes searching and tracking of a target based on bionics with large-range scanning. This sensor system imitates compound eye of an insect where every infrared sensor is a small eye. Actual engineering application adopts 4 infrared sensor constructs in a $2 * 2$ array shown in Fig. 1. Obviously, after the view field of every small eye is put together, the sensing range is extended as far as possible.

2.1.1 Acquisition of 2D measurement information

In this system, regard the observed center as a datum mark. First, define global coordinates. Because the IRST system is mostly used to track a long-distance target (distance $r \geq 15$ km), the observation platform is approximated as a point. Under this circumstance, still select the center of the spherical base as the global coordinates' origin. For Cartesian coordinates' definition, the platform centerline pointing to fore-side is selected as y -axis, and the right direction vertical to the y -axis is chosen as

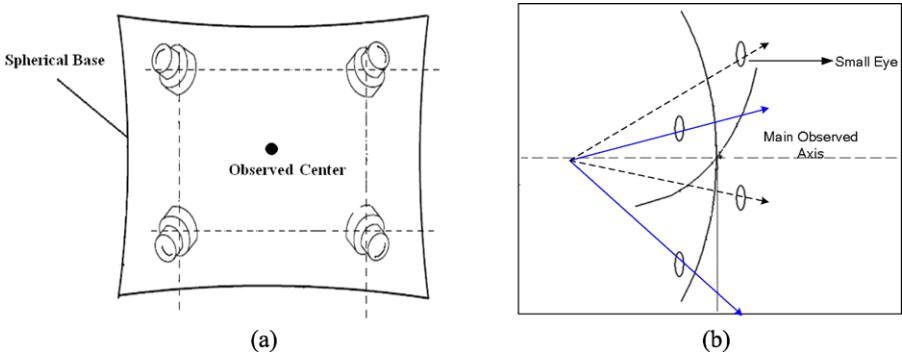
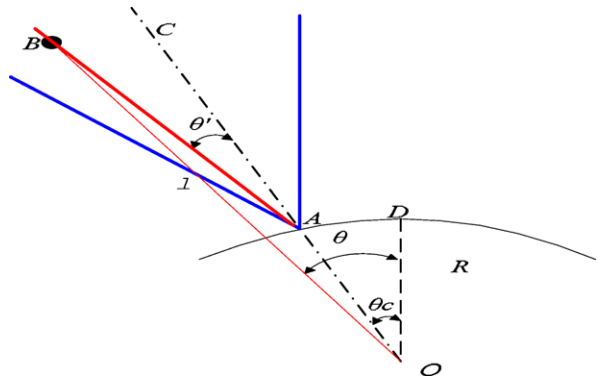


Fig. 1 Sensor system: (a) compound eye construction and (b) field of view of compound eye

Fig. 2 Principle of transforming coordinates



x -axis. Correspondingly, the upward direction vertical to the x - y plane is selected as z -axis.

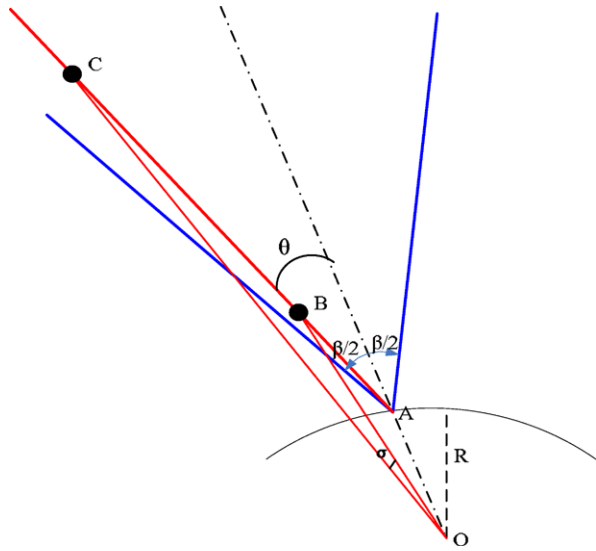
For each small eye, the 2D angle offset away from main observed axis listed in Fig. 1(b) is constant. Denote these angle offsets as $(\theta_{ccd}^i, \varphi_{ccd}^i)'$ where $i = 1, 2, \dots, count$, and $count = 4$ being the number of small eyes. For each local small eye, suppose that its valid image plane is rectangular, the focus is f and the distance of each pixel is h . Moreover, regard the center of the image plane for each eye as the local coordinates' origin. Define the horizontal to the right as positive X -axis and the vertical to upward as positive Y -axis in 2D bearing-only coordinates. Their unit is also a pixel. Suppose that the coordinates of the certain target are (n_x, n_y) . Denote the azimuth angle and the pitching angle in local coordinates as θ' and φ' . Then [7]

$$\theta' \doteq \frac{n_x \bullet h}{f}, \tag{1}$$

$$\varphi' \doteq \frac{n_y \bullet h}{f}. \tag{2}$$

In order to explain the rationality of defined coordinates and simplify calculations, we give a principle explanation listed as Fig. 2 in bearing-only coordinates.

Fig. 3 The coordinate transformation of different targets



In Fig. 2, we give a principle of transforming coordinates about an azimuth angle. For pitching angle, the principle is similar. Here, O is the center of the spherical base of the platform and OD is the datum line of the global azimuth angle. Moreover, A is the installed position of a small eye. AC is its optical axis. B is the position of a target. θ' is the azimuth angle in the local coordinates, and θ is the azimuth angle in the global coordinates. When the target is a far away observation point ($R \ll l$), there is an approximate equation

$$\theta \approx \theta_c + \theta', \tag{3}$$

where

$$\theta_c = \theta_{ccd}^i + \hat{\theta} \tag{4}$$

with $\hat{\theta}$ being the horizontal angle between the local axis and the global axis, and θ_{ccd}^i being the installed position (azimuth angle) in global coordinates.

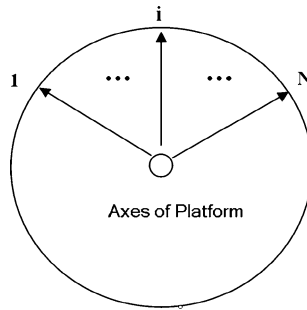
The following study is a real problem. There are two targets (B and C) whose distances away from the observation point are different and shown in Fig. 3. Then studying their transformed coordinates by the above approach can guarantee the range of allowable error. By simulation, this approximation is considered trustworthy when target B is 150 m away from the observation point [7]. Obviously, this coordinate transformation can provide enough accuracy.

2.2 Platform design

In order to search and track maneuvering target in all airspace area, sensor platform needs to go round and round.

Here, platform design adopts a rotating and gazing pattern. It indicates that sensor platform needs to stop intermittently to gaze in the course of rotating. The aim of gaze is to receive sufficient target radiation energy and to ensure the reliability of

Fig. 4 The scanning principle of a sensor platform



observation images. As shown in Fig. 4, observing target is done in small sectors and $1, 2, \dots, N$ are gazing points. Platform rotates in a circle as a scanning cycle T with tracking processing.

3 Definition of state

Generally, the IRST system has high sampling frequency and denotation precision, which is usually milli-radian level. Thus, target state movement is approximately linear. Based on this premise, we specify the 2D polar coordinates as tracking coordinates. Define the state variable by

$$\zeta = [\theta_i \quad \dot{\theta}_i \quad \ddot{\theta}_i \quad \varphi_i \quad \dot{\varphi}_i \quad \ddot{\varphi}_i]. \tag{5}$$

Denote the measurement matrix by

$$z = [\theta \quad \varphi]. \tag{6}$$

Suppose that there are N targets in clutter environment. Then, the state and measurement equations are

$$\begin{cases} \zeta^t(k) = \Phi^t(k-1)\zeta^t(k-1) + \vartheta^t(k-1), \\ z_j(k) = H(k)\zeta^t(k) + \nu(k), \end{cases} \tag{7}$$

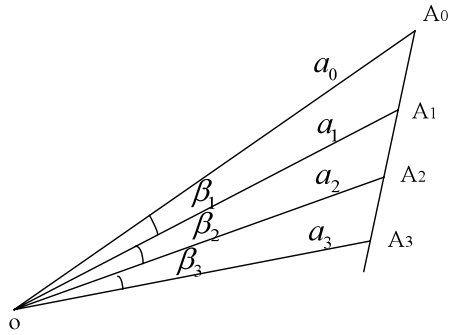
$t = 1, \dots, N; \quad j = 1, 2, \dots, m_k,$

where $\zeta^t(k)$ denotes the state matrix of target t at time k , and $z_j(k)$ denotes the j th measurement matrix. $\Phi^t(k-1)$ and $H(k)$ are linear system matrices. The state noise $\vartheta^t(k-1)$ and the angle measurement noise $\nu(k)$ are all Gaussian white noise with zero mean, and they are also uncorrelated, with covariance matrices are $\Theta(k)$ and $R(k)$, respectively.

4 Adaptive gate technology

Associated gate is an important technology which affects the association effects and the tracking performances. The bad association might lead to the results of an uncertain calculation and missing the real measurements. The traditional gate technology

Fig. 5 Angle change of target motion



is inefficient in the $\theta-\phi$ plane. They not only cannot limit false track overextension with the dense clutter but also hardly confirm those real target tracks. We will give an gate technology to perform the point to point association that is track initiation. For point to track association, the real system adopts a constant rectangular gate.

Firstly, the initial gate will be designed to confirm isolated measurement. Gate technology in the $\theta-\phi$ plane must be based on the characteristic of bearing-only target motion. Obviously, the nearer is target motion, the larger is angle measurement change. Thus, the area of confirming measurement must have good adaptability. In view of these factors, rational gate design is core for track processing in bearing-only tracking. Under normal circumstances, tracking systems require that targets be reliably tracked at D_{\min} kilometers away from the observation point. Design initial gate as the rule

$$\left\| \frac{z_i(k+1) - z_j(k)}{t_{k+1} - t_k} \right\| \leq \frac{v_{\max}}{D_{\min} * 10^3} \tag{8}$$

where t_k is k th sample time.

Combining with the angle change analysis of bearing-only target motion, the gate of extrapolating by using linear and second-order polynomials will be presented. As shown in Fig. 5, suppose that the observation point is O and target moves along A_0A_3 in a straight line. The sample points of the moving target at every sample time are $A_0, A_1, A_2, A_3, \dots$ and the distances of the different sample points away from observation point are $a_0, a_1, a_2, a_3, \dots$. The angles between the observation point and the sample points are $\beta_1, \beta_2, \beta_3, \dots$. Due to the assumption that the sampling time of a passive sensor is shorter and the target confirming accuracy is high enough, the average velocity of the adjacent sampling circle is approximately equal and target motion is an approximately straight line form. Simultaneously, the angle change in the $\theta-\phi$ plane is small. If we suppose that A_2 corresponds to the sampling time k , equations can be established based on the triangular relationship according to Fig. 6. Simplify those equations, we get the result as

$$\frac{\Delta t_{k-2}^{k-1} \cdot a_2}{\Delta t_{k-2}^k \cdot a_1} = \frac{\sin \beta_1}{\sin(\beta_1 + \beta_2)} \approx \frac{\beta_1}{\beta_1 + \beta_2}, \tag{9}$$

where Δt_i^j denotes the time interval between sample time i and sample time j . Then

$$\begin{aligned} \left(\beta_2 - \frac{\beta_1}{\Delta t_{k-2}^{k-1}} \cdot \Delta t_{k-1}^k \right) &\approx \left[\frac{\Delta t_{k-2}^k}{\Delta t_{k-2}^{k-1}} \cdot \frac{a_1}{a_2} - \frac{\Delta t_{k-1}^k}{\Delta t_{k-2}^{k-1}} - 1 \right] \cdot \beta_1 \\ &\leq \left(\frac{\Delta t_{k-2}^k}{\Delta t_{k-2}^{k-1}} \cdot \frac{D_{\min}}{D_{\min} - v_{\max} \cdot \Delta t_{k-1}^k} - \frac{\Delta t_{k-1}^k}{\Delta t_{k-2}^{k-1}} - 1 \right) \cdot \beta_1. \end{aligned} \tag{10}$$

Formula (10) denotes the upper limit of angle deviation when a candidate track is linearly extrapolated in the $\theta-\varphi$ plane. Now use the upper limit as linearly extrapolating association gate in the course of track initiation. Make the assumption that the measurement $z_i(k)$ and the j th component of the vector $\hat{z}_m^L(k)$ is obtained by extrapolating candidate track m . If the following formula is satisfied, the measurement $z_i(k)$ will be confirmed:

$$\begin{aligned} &|z_{i,j}(k) - \hat{z}_{m,j}^L(k)| \\ &\leq \left| \left(\frac{\Delta t_{k-2}^k}{\Delta t_{k-2}^{k-1}} \cdot \frac{D_{\min}}{D_{\min} - v_{\max} \cdot \Delta t_{k-1}^k} - \frac{\Delta t_{k-1}^k}{\Delta t_{k-2}^{k-1}} - 1 \right) \cdot (z_{k-1,i} - z_{k-2,i}) \right|. \end{aligned} \tag{11}$$

When extrapolating candidate track using a second-order polynomial, suppose that A_3 corresponds to the sampling time k . Then, equations are established based on the triangular relationship. We simplify those equations and get the result as

$$\frac{\Delta t_{k-2}^{k-1} a_3}{\Delta t_{k-2}^k a_2} = \frac{\sin \beta_2}{\sin(\beta_2 + \beta_3)} \approx \frac{\beta_2}{\beta_2 + \beta_3}. \tag{12}$$

Then

$$\begin{aligned} \beta_3 &- \left[\left(\frac{\beta_2}{\Delta t_{k-2}^{k-1}} + \Delta t_{k-2}^{k-1} \cdot \frac{\frac{\beta_2}{\Delta t_{k-2}^{k-1}} - \frac{\beta_1}{\Delta t_{k-3}^{k-2}}}{\Delta t_{k-3}^{k-1}} \right) \cdot \Delta t_{k-1}^k + \frac{\frac{\beta_2}{\Delta t_{k-2}^{k-1}} - \frac{\beta_1}{\Delta t_{k-3}^{k-2}}}{\Delta t_{k-3}^{k-1}} \cdot (\Delta t_{k-1}^k)^2 \right] \\ &= \left(\frac{a_2 \cdot \Delta t_{k-2}^k}{a_3 \cdot \Delta t_{k-2}^{k-1}} - \frac{\Delta t_{k-1}^k}{\Delta t_{k-2}^{k-1}} - \frac{\Delta t_{k-1}^k}{\Delta t_{k-3}^{k-1}} - \frac{(\Delta t_{k-1}^k)^2}{\Delta t_{k-2}^{k-1} \cdot \Delta t_{k-3}^{k-1}} - 1 \right) \cdot \beta_2 \\ &\quad + \frac{\Delta t_{k-1}^k \cdot \Delta t_{k-2}^{k-1} + (\Delta t_{k-1}^k)^2}{\Delta t_{k-3}^{k-1} \cdot \Delta t_{k-3}^{k-2}} \cdot \beta_1 \\ &\leq \left(\frac{\Delta t_{k-2}^k}{\Delta t_{k-2}^{k-1}} \cdot \frac{D_{\min}}{D_{\min} - v_{\max} \cdot \Delta t_{k-1}^k} - \frac{\Delta t_{k-1}^k}{\Delta t_{k-2}^{k-1}} - \frac{\Delta t_{k-1}^k}{\Delta t_{k-3}^{k-1}} \right. \\ &\quad \left. - \frac{(\Delta t_{k-1}^k)^2}{\Delta t_{k-2}^{k-1} \cdot \Delta t_{k-3}^{k-1}} - 1 \right) \cdot \beta_2 + \frac{\Delta t_{k-1}^k \cdot \Delta t_{k-2}^{k-1} + (\Delta t_{k-1}^k)^2}{\Delta t_{k-3}^{k-1} \cdot \Delta t_{k-3}^{k-2}} \cdot \beta_1. \end{aligned} \tag{13}$$

Formula (13) denotes the upper limit of the angle deviation when a candidate track is extrapolated in the $\theta-\varphi$ plane using a second-order polynomial. Use the upper limit

as a second-order extrapolating association gate in the course of track initiation. If the following formula is satisfied, the measurement will be confirmed:

$$\begin{aligned}
 |z_{i,j}(k) - \hat{z}_{m,j}^R(k)| \leq & \left| \left(\frac{\Delta t_{k-2}^k}{\Delta t_{k-2}^{k-1}} \cdot \frac{D_{\min}}{D_{\min} - v_{\max} \cdot \Delta t_{k-1}^k} - \frac{\Delta t_{k-1}^k}{\Delta t_{k-2}^{k-1}} \right. \right. \\
 & \left. \left. - \frac{\Delta t_{k-1}^k}{\Delta t_{k-3}^{k-1}} - \frac{(\Delta t_{k-1}^k)^2}{\Delta t_{k-2}^{k-1} \cdot \Delta t_{k-3}^{k-1}} - 1 \right) \cdot (z_{k-1,i} - z_{k-2,i}) \right. \\
 & \left. + \frac{\Delta t_{k-1}^k \cdot \Delta t_{k-2}^{k-1} + (\Delta t_{k-1}^k)^2}{\Delta t_{k-3}^{k-1} \cdot \Delta t_{k-3}^{k-2}} \cdot (z_{k-2,i} - z_{k-3,i}) \right|, \quad (14)
 \end{aligned}$$

where $\hat{z}_{m,j}^R(k)$ is the j th component of the vector $\hat{z}_m^R(k)$ which is obtained by extrapolating candidate track m using a second-order polynomial. These gate technologies take full advantage of the characteristic of bearing-only target motion, and the association gate adaptively adjusts according to the measurements of the different candidate track.

5 Multi-model bearing-only tracking

5.1 Multi-model algorithm. Introduction

It is well known that the good performance of Kalman filtering must be based on a suitable target model. In the course of study and engineering application of bearing-only maneuvering target tracking, the tracking performance of a single model based adaptive filter isn't so good. Its limitation is mainly the competition between tracking accuracy and rapid response to target tracking. Especially regarding bearing-only tracking, for its higher target maneuverability and the variety of structures and parameters existing in a target motion model, the single-model adaptive filter has difficulties to accurately recognize these varieties in time so that inaccurate model and false tracking appear. Multi-model filters use several appropriate models to approximate the real target motion. Among them each model has a potential maneuvering mode. Random maneuvering of target is depicted as random hopping among models. By designing a filter composed of several models, we accordingly carry them into effective execution for maneuvering target tracking. Thus, improving tracking performance is naturally shown. If we make an assumption that random hopping of target motion model state is discrete and target motion state is continuous, maneuvering target tracking is a typical mixed estimation problem. The traditional solution of a mixed estimation problem is combining estimation with decision-making. When making a hard decision for the uncertain parameter and structure, the estimation result is usually bipolar optimization rather than global optimization. Under these circumstances, the multi-model approach nowadays becomes the main solution to mixed estimation.

The basic idea of multi-model maneuvering target tracking approach is mapping a potential motion model into a model set. Each model in this set represents different maneuvering mode, and the varieties of models based filter works in parallel. State

estimation output is Bayesian illation based data fusion of all filtering state estimates. Suppose that $i \in \{1, 2, \dots, (M_s)^k\}$ is a model state sequence indexed up to time k , and M_s is the model number in the model set. Simultaneously, $\hat{x}_i(k|k)$ and $P_i(k|k)$, respectively, are the state estimate and the error covariance under the assumption of the model state sequence m^k matching model sequence m_i^k of index i . $P\{m^k = m_i^k | z^k\}$ is the posterior probability of this assumption. S^k is a set of all potential model sequences. Z^k is the measurement sequence. Then, the optimal multi-model estimation under LMSE need to consider all potential model state sequences assumption, namely

$$\begin{cases} \hat{x}(k|k) = \sum_{m_i^k \in S^k} \hat{x}_i(k|k) P\{m^k = m_i^k | Z^k\}, \\ P(k|k) = \sum_{m_i^k \in S^k} \{P_i(k|k) + (\hat{x}(k|k) - \hat{x}_i(k|k))(\hat{x}(k|k) - \hat{x}_i(k|k))'\} \\ \quad \times P\{s^k = m_i^k | z^k\}. \end{cases} \quad (15)$$

Apparently, the number of potential model sequences assumption presents an index growth with flowing time. It produces an unacceptable computation cost. Especially disadvantageous is that target threat degree can't be estimated due to lacking distance information in passive tracking system, so real-time is very important to this system. Thus, the computation cost of the selective approach must satisfy the demand of a tracking operation. The IMM algorithm [8–10] proposed by H.A.P. Bolm is an inferior optimized multi-model algorithm which is highly cost-effective. This algorithm makes an assumption that transformation of different models obeys a finite Markov chain with known transition probability. It has the same performance as GBP2 and the advantage of computation cost over GBP1. IMM is regarded as the first multi-model algorithm up to application value [11].

5.2 IMM algorithm based on bearing-only measurement

Assume that target motion can be depicted as a model from r assumption models in some time, denote the model set as $M_r := \{1, \dots, r\}$. The effective event of model j is denoted by $M^j(k)$ in the sampling period $(t_{k-1}, t_k]$. For the assumption model j , the target state equations are

$$\begin{cases} X(k) = F^j(k-1)X(k-1) + G^j(k-1)W^j(k-1), \\ Z(k) = H^j(k)X(k) + V^j(k). \end{cases} \quad (16)$$

Assume that the probability of model j is

$$\mu^j(0) = \Pr\{M^j(0)\}. \quad (17)$$

The transition probability is

$$p_{ij} = \Pr\{M^j(k) | M^i(k-1)\}. \quad (18)$$

It is known and provided by the Markov chain jump from $M^j(k-1)$ to $M^j(k)$ in this time.

1. Mixed probability calculation

If $M^j(k)$ and the measurement set $Z_{k-1} (Z_{k-1} := \{Z(1), Z(2), \dots, Z(k-1)\})$ are known in sampling time k , the appearance probability of M^i can be expressed as

$$u^{ij}(k-1|k-1) = P\{M(k-1) = M_i | M(k) = M_j, Z_{k-1}\} = \frac{1}{c_j} p_{ij} u^i(k-1), \tag{19}$$

where $i, j = 1, 2, \dots, n$, and c_j is a normalization constant.

2. Interacting and mixed calculation

It gives the calculating expression of $\hat{X}^i(k-1|k-1)$ and corresponding covariance $P^i(k-1|k-1)$ for different models:

$$\begin{cases} \hat{X}^{0j}(k-1|k-1) = \sum_{i=1}^n \hat{X}^i(k-1|k-1) u^{ij}(k-1|k-1), \\ P^{0j}(k-1|k-1) = \sum_{i=1}^n u^{ij}(k-1|k-1) \{P^i(k-1|k-1) + [\hat{X}^i(k-1|k-1) - \hat{X}^{0j}(k-1|k-1)][\hat{X}^i(k-1|k-1) - \hat{X}^{0j}(k-1|k-1)]'\}. \end{cases} \tag{20}$$

3. Model conditional filtering

Regard the obtained mixed initial condition from step 2 and the current measurement $Z(k)$ as input of each filter at time k . Thus, we figure out a new model estimate, i.e., $\hat{X}^j(k|k)$ and $P^j(k|k)$. Together with the predicted measurement $\hat{Z}^j(k|k-1)$ and the corresponding innovation covariance $S^j(k)$, we figure out the likelihood function of the filter

$$\begin{aligned} \Lambda^j(k) &= \frac{1}{\sqrt{2\pi|S^j(k)|}} \\ &\times \exp\left\{-\frac{1}{2}[Z(k) - \hat{Z}^j(k|k-1)]'(S^j(k))^{-1}[Z(k) - \hat{Z}^j(k|k-1)]\right\}, \end{aligned} \tag{21}$$

where the function distribution is Gaussian.

4. Renewing model probability

Each renewing model probability is as follows:

$$u^j(k) = \frac{1}{c} \Lambda^j(k) \sum_{i=1}^n p_{ij} u^i(k-1). \tag{22}$$

5. State and covariance estimates

Formulas of state and covariance estimates are:

$$\begin{cases} \hat{X}(k|k) = \sum_{j=1}^n \hat{X}^j(k|k) u^j(k), \\ P(k|k) = \sum_{j=1}^n u^j(k) \{P^j(k|k) + [\hat{X}^j(k|k) - \hat{X}(k|k)][\hat{X}^j(k|k) - \hat{X}(k|k)]'\}. \end{cases} \tag{23}$$

By an analysis of algorithm framework, measurement information utilization of IMM exists in not only filtering estimate but also in model probability. And IMM can adaptively adjust the model by a model probability change. Simultaneously, this algorithm has modularization characteristic. Through different applications, the filtering module can adopt all kinds of linear and nonlinear filtering algorithms. Finally, efficiency is improved by virtue of each filtering module working side by side in this algorithm.

5.3 Model selection for bearing-only tracking

In this paper, the model selection is only limited to CV and CA because the performance for CT in polar coordinates isn't so good and the value of ω is difficult to grasp. The reason is mainly based on the hypothesis that the data sampling rate of IRST system is high enough. The research indicates that general motion can be approximated by a certain combination of CV and CA. But until now, the relative theories about model selection for MM filter are still lacking.

5.4 Positive definiteness of inverse matrix and elimination of ill-posed matrix

In the course of target tracking, many inverse matrices such as that of filtering covariance matrix need to be computed. These matrixes are positive definite in theory. However, for the reason of finite word length of computers, error is accumulated with time so that the filtering covariance matrixes lose the features of positive definiteness and symmetry. Obviously, filtering divergence will appear and it will lead to missed tracking. Moreover, an ill-posed matrix might appear. When solving for its inverse, the results are very unstable. Filtering divergence will also appear. Solution in the engineering application is shown as follow:

1. Positive definiteness

According to the conditions of being positive definite, first, compel the matrix to symmetry. Then, resolve to get its eigenvalue and determine if they are positive or negative. When all eigenvalues are positive, do nothing and go on. If there is a negative eigenvalue, the matrix isn't positive definite. Under this circumstance, add to all diagonal elements of the matrix an appropriate positive number. Continue the process till the matrix is positive definite.

2. Elimination of ill-posed matrix

First, resolve to get the eigenvalues of the matrix. Then decide if a certain eigenvalue is close to zero. If so, the matrix is ill-posed, else continue the operation. In this tracking processing system, the diagonal elements of the matrix will be changed by adding an appropriate number W , where $W \in [2, 5]$. The process will go on till the ill-posed matrix is eliminated.

6 The processing of suspected threatening target

According to the characteristic of bearing-only tracking, the estimation of threatening target is very important when lacking distance information. The most intuitive

feeling is that suspected threatening target is one whose attacking velocity is high and attacking angle change is small. These stationary targets need to be tracked first and foremost. In real application, if (24) is satisfied in three consecutive scan cycles for the estimation state of the target, it is considered as a threatening target and target threat degree is upgraded:

$$\|(\kappa_{k+1} - \kappa_k)/(t_{k+1} - t_k)\| \leq \omega_T \tag{24}$$

where κ_k is the bearing-only position vector at sample time k and ω_T is threatening decision angle given by the system.

Moreover, confidence measure based on this decision is not high. Here, some additional information from the passive sensor can be used, for example, gray change information, area change information, etc. Using of this information can improve threat estimation precision to some extent.

7 Simulation

Assume that measurement noise is Gaussian white noise whose coefficient is 1 milli-rad ($\text{rad} \times 10^{-3}$). In this tracking filtering algorithm, the approach of direct angle modeling is chosen. There is an IMM filter composed of 3 models used to track. These models are depicted as follows. There are different Q matrices for model 1 and model 2, which are CV with state noise coefficients of 1 and 0.1, respectively, and model 3 is chosen as CA whose state noise coefficient is 0.1. Clutter density is Poisson distributed and $\lambda = 1.5198 \times 10^{-6}$) milli-rad². The initial model probability matrix is

$$\mu_0 = \begin{bmatrix} \frac{1}{3} & \frac{1}{3} & \frac{1}{3} \end{bmatrix}. \tag{25}$$

The model transition probability matrix is

$$P = \begin{bmatrix} 0.98 & 0.01 & 0.01 \\ 0.01 & 0.98 & 0.01 \\ 0.01 & 0.01 & 0.98 \end{bmatrix}. \tag{26}$$

Ten selective maneuvering targets are shown in Fig. 6 in the polar coordinates and the initial states of those targets are listed in Table 1. The tracking effects are shown in Fig. 7 where the coordinates, horizontal and vertical axes, respectively, are in azimuth ($\text{rad} \times 10^{-3}$) and pitch ($\text{rad} \times 10^{-3}$). The tracking errors are shown in Fig. 8 where the coordinates, horizontal and vertical axes, respectively, are in circle number (N) and $\text{rad} \times 10^{-3}$. Here, we make an assumption that $T = 1.5$ s, and the sampling number is $N = 60$.

8 Engineering application

Aiming at the research system, we design a platform to test its application. In a real system, the searching platform is a sphere whose diameter is about 60 cm. There are

Fig. 6 The target tracks in the polar coordinates

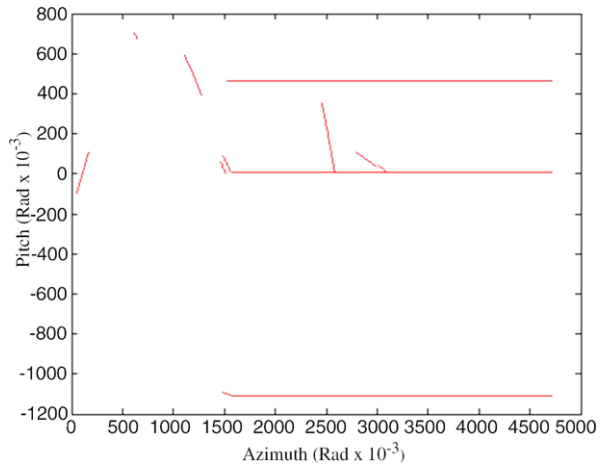


Table 1 The initial states of the targets

Target	Initial X Position r_x (m)	Initial X Velocity v_x (m/s)	Initial Y Position r_y (m)	Initial Y Velocity v_y (m/s)	Initial Z Position r_z (m)	Initial Z Velocity v_z (m/s)
1	-50000	50	3000	40	700	15
2	10000	30	20000	250	15000	35
3	20000	15	1000	30	-2000	50
4	0	15	10000	30	-20000	-50
5	-20000	30	3000	40	700	15
6	3000	30	50000	20	150	35
7	-8000	-15	5000	30	100	50
8	0	20	20000	100	10000	50
9	0	30	20000	100	100	30
10	80000	200	60000	100	80000	250

4 infrared cameras that are mounted on the sphere surface in a $2 * 2$ array. There are 3 gazing points at intervals of 30 degrees. The cycle T , which is the time of the platform to complete a circle, is 3.7 s. The interval among gazing points is 0.6 s. Moreover, measurement noise is Gaussian white noise. The noise coefficient is 0.01. The sensor detecting probability is $P_D = 0.99$. The gate coefficient is $P_G = 0.999$.

Select three models as elements of the IMM. Model 1 and model 2 are CV. Model 3 is CA. The initial model probability matrix is

$$\mu_0 = \begin{bmatrix} \frac{1}{3} & \frac{1}{3} & \frac{1}{3} \end{bmatrix}.$$

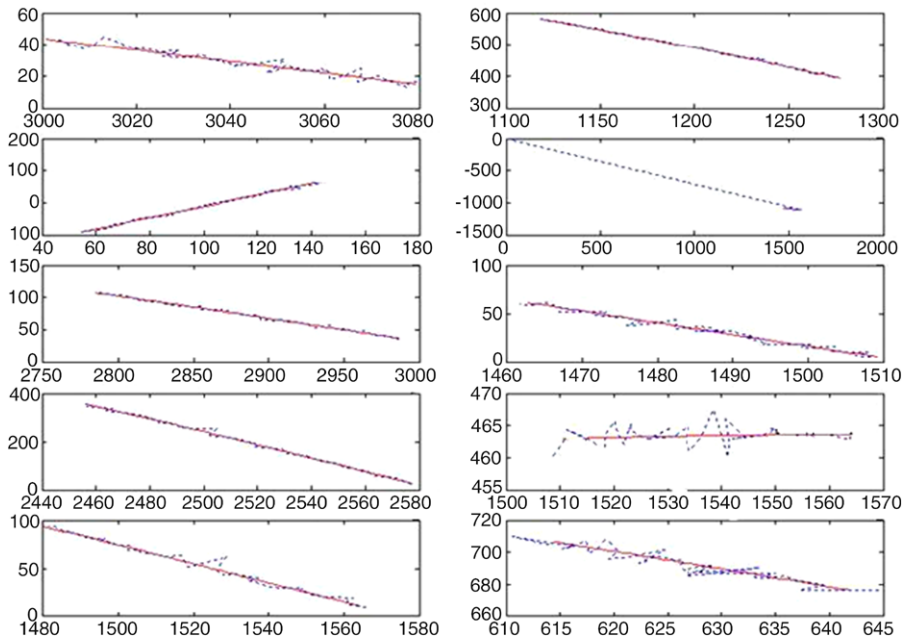


Fig. 7 The tracking effects

The model transition probability matrix is

$$P = \begin{bmatrix} 0.98 & 0.01 & 0.01 \\ 0.01 & 0.98 & 0.01 \\ 0.01 & 0.01 & 0.98 \end{bmatrix}.$$

The noise coefficients of their processes are 0.5, 1 and 0.01, respectively. The actual tracking effect of the engineering application is shown in Fig. 9.

9 Conclusions

According to simulation results of the whole track processing system, the solutions presented in this paper are suitable for bearing-only tracking based on bionics with theIRST system. There is also a clear conclusion that tracking accuracy is improved by using IMM. On the other hand, algorithm complexity is enhanced indeed, and that computation cost is in direct proportion to the number of models. Under the accuracy condition, choose the number of models as small as possible. By simulation, we draw a conclusion: If the number of CV models exceeds 3 or the number of CA exceeds 2, minimal performance improvement is displayed in the bearing-only tracking with computation cost greatly increased. This is due to too much unnecessary model competition in the multi-model data fusion. Excessive use of the models not only increases computation cost but also reduces the accuracy of estimation. Based

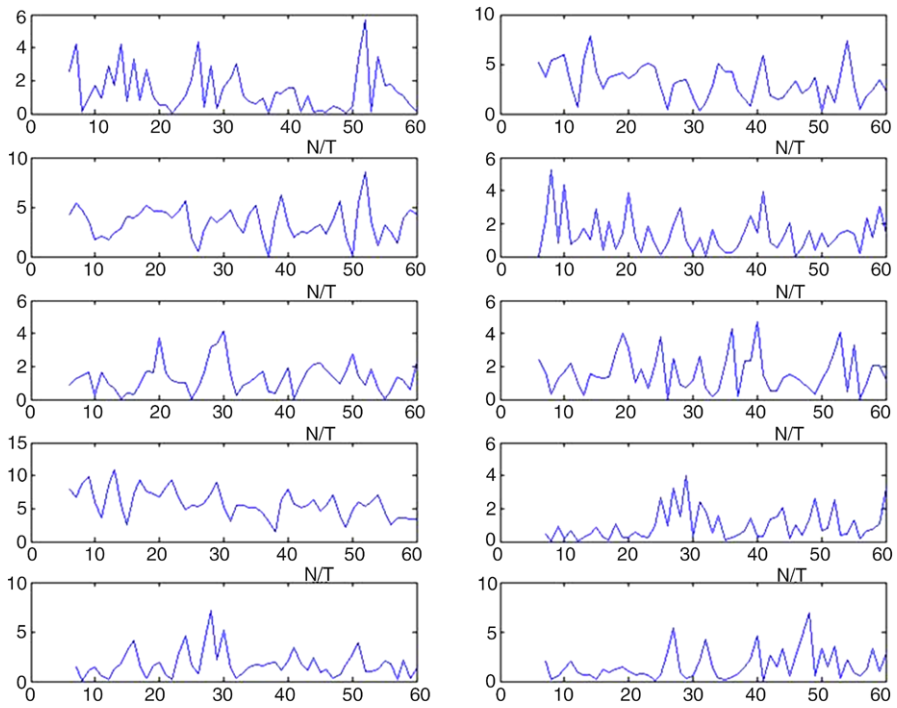


Fig. 8 The tracking errors

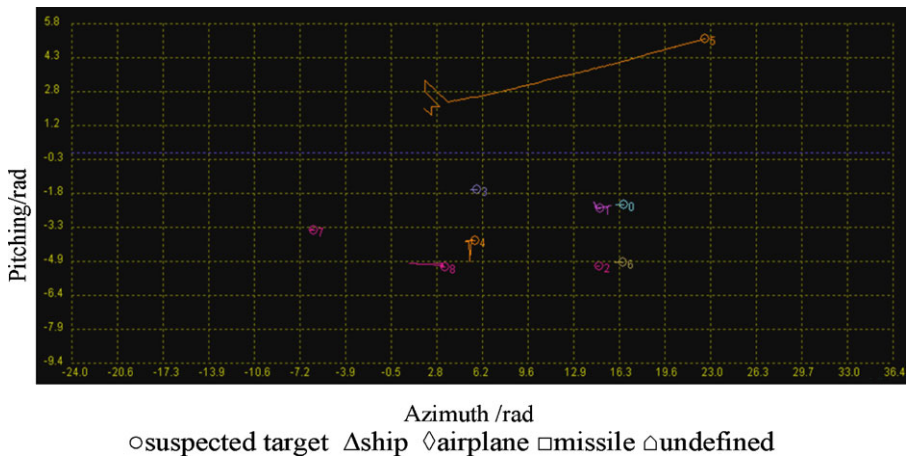


Fig. 9 The actual tracking effect of the engineering application

on simulation, balancing the two factors, accuracy and computation cost, by choosing two CV and one CA to compose a multi-model tracking filter, we can get more satisfactory results. Finally, in the actual test of engineering application environment, the performance of the tracking system has to be preliminarily validated. But the cy-

cle control of the platform rotation limits the tracking effect to some extent. Tracking cycle T decreases with platform rotating time. In order to get good tracking effect, T needs to be as short as possible. Yet, considering matched gazing control and large moment of inertia of the platform, platform control is very difficult to complete precisely. Moreover, these tracking algorithms are still expected to be improved. There are many improvements for characteristic of bearing-only tracking. But they are out of the scope of this paper.

Acknowledgements The authors thank Senior Professor Yue Lou, Engineer Wei Zhang, Dr. Chen Li in preparing simulation data and completing final open-air test. This work is supported by the National Natural Science Foundation of China (Grant No. 61005026) and the Gansu Provincial Science and Technology Planning of China (Grant No. 0916RJZA017).

References

1. Popp RL, Pattipati KR, Bar-Shalom Y (2001) m-Best S-D assignment algorithm with application to multitarget tracking. *IEEE Trans AC* 37(1):22–38
2. Fogel E, Gavish M (1998) N th-order dynamics target observability from angle measurements. *IEEE Trans AES* 3(24):305–307
3. Mangzuo S (1995) Range information extraction from tracking data using object kinematic parameters. *SPIE* 2561:484–488
4. Kronhamn TR (1998) Bearings-only target motion analysis based on a multi-hypothesis Kalman filter and adaptive oweship motion control. *IEE Proc Radar, Sonar Navig* 145(4):247–252
5. Pattipati KR, Deb S, Bar-Shalom Y et al (1992) A new relaxation algorithm and passive sensor data association. *IEEE Trans AC* 37(2):98–213
6. Chen H, Li C (2010) Data association approach for two dimensional tracking based on bearing-only measurements in clutter environment. *J Softw* 5(3):336–343
7. Lou Y, Zhu H, Li C et al (2006) Key technology report of multi-target tracking fusion system
8. Metropolis N, Rosenbluth AW, Rosenbluth MN et al (1953) Equations of state calculations by fast computing machines. *J Chem Phys* 21(6):1087–1091
9. Kong A, Liu JS, Wong WH (1994) Sequential imputations and Bayesian missing data problem. *J Am Stat Assoc* 89(425):278–288
10. Gordon NJ, Salmund DJ, Smith AFM (1993) Novel approach to nonlinear-non-Gaussian Bayesian state estimation. *IEE Proc F*, 140(2):107–113
11. Johnston LA, Krishnamurthy V (2001) An improvement to the interacting multiple model (IMM) algorithm. *IEEE Trans Signal Process* 49:2909–2923